24th INTERNATIONAL CONGRESS ON SOUND AND VIBRATION
23–27 July 2017, London

PARAMETER IDENTIFICATION OF AGRICULTURAL TIRE BY USING RIGID RING MODEL

Katsuhide Fujita

National Institute of Technology, Ube College, Dept. of Mechanical Engineering, Ube, Yamaguchi, JP
email: katuhide@ube-k.ac.jp

Takashi Saito

Yamaguchi University, Graduate School of Science and Technology for Innovation, Ube, Yamaguchi, JP,

Mitsugu Kaneko

Yanmar Co., Ltd., Research and Development Center, Maibara, Shiga, JP,

The objective of this study is to clarify the vibration generation mechanism of agricultural machinery caused by the interaction between the tire lugs and the road surface. It is important to investigate the lug excitation force occurring on a rolling agricultural tire in order to clarify the vibration generation mechanism. In our previous study, it is confirmed that the dynamic behavior of rolling tire is influenced by the vibration characteristics of the tire and only the rigid modes can affect the rolling tire behavior. Therefore, we modeled the agricultural tire as a rigid ring tire model (SWIFT model) in order to estimate the lug excitation force. As for agricultural tire, out-of-plane dynamics is also important due to cross-stich lugs. This model can describe not only in-plane tire dynamics but also out-of-plane tire dynamics. An important aspect of tire modelling is the identification of the tire model parameters. As for model parameter identification, few studies have been carried out to identify out-of-plane parameters, while many studies were done with regard to in-plane parameters. In this research, the equations of motion of the rigid ring model are derived and calculation procedure for obtaining the natural frequencies of the rigid ring model is formulated. Furthermore, the model parameters are identified by minimizing the difference between measured and calculated natural frequencies using Downhill Simplex method. The natural frequencies and natural modes predicted by the calculation using the identified model parameters show good agreement with those obtained experimentally.
Keywords: agricultural tire, rigid ring model, identification, lug excitation force

1. Introduction

In Japan, expansion of farm management scale is promoted in order to perform efficient and stable farm management. This tendency increases the opportunity when tractor runs on pavement. Therefore, the speedup of tractor is expected. As a result, the speedup causes the increase of vibration and noise. Generally, agricultural tires have high and large cross-stitch lug. So, lug excitation force is primary cause of vibration during running on pavement. The objective of this study is to clarify the vibration generation mechanism caused by tire lugs. It is important to evaluate lug excitation force.

In our previous study, it is confirmed that the dynamic behaviour of rolling tire is influenced by the vibration characteristics and only the rigid modes can affect the rolling tire behaviour [1,2]. Therefore, we modelled the agricultural tire as in-plane rigid ring model and the lug excitation forces occurring on a rolling tire are identified as for vertical and longitudinal direction [3]. However, as for an agricultural tire, lateral direction lug excitation force also generates due to cross-stitch lugs. In order to estimate lateral force, the rigid ring model to describe the out-of-plane tire dynamic is required. The rigid ring tire model (SWIFT model), which is introduced by Pacejka,H.B is able to describe dynamic tire behaviour for in-plane and out-of-plane motion. At that time, an important aspect of tire modelling is the identification of the model parameters. As for tire model parameters identification, few studies have been carried out to identify out-of-plane parameters, while many studies were done with regard to in-plane parameters. In this research, the equations of motion of the SWIFT model are derived and the equations of motion are rearranged to describe the in-plane and the out-of-plane dynamics. From the rearranged equations of motion, frequency equations are derived separately and calculation procedure for obtaining the natural frequencies of the rigid ring model is formulated. Furthermore, the model parameters are identified by minimizing the difference between measured and calculated natural frequencies using Downhill Simplex method. The natural frequencies and natural modes predicted by the calculation using the identified model parameters show good agreement with those obtained experimentally.

2. Modelling of agricultural tire

2.1 Rigid ring model

The rigid ring model is based on the research of Zegelaar, P.W.A.[4] and Maurice, J.P.[5] and this model is referred to as the SWIFT (Short Wavelength Intermediate Frequency Tire) model proposed by Pacejka, H.B.[6]. This model represents a pneumatic tire-wheel system and consist of four components : the tire tread-band, the tire sidewalls with pressurized air, the wheel and a contact model as shown in Fig. 1. The tread-band is modelled as a rigid circular ring and the wheel as a rigid body. The tread-band and the wheel are connected through sidewalls with pressurized air three-dimensionally.

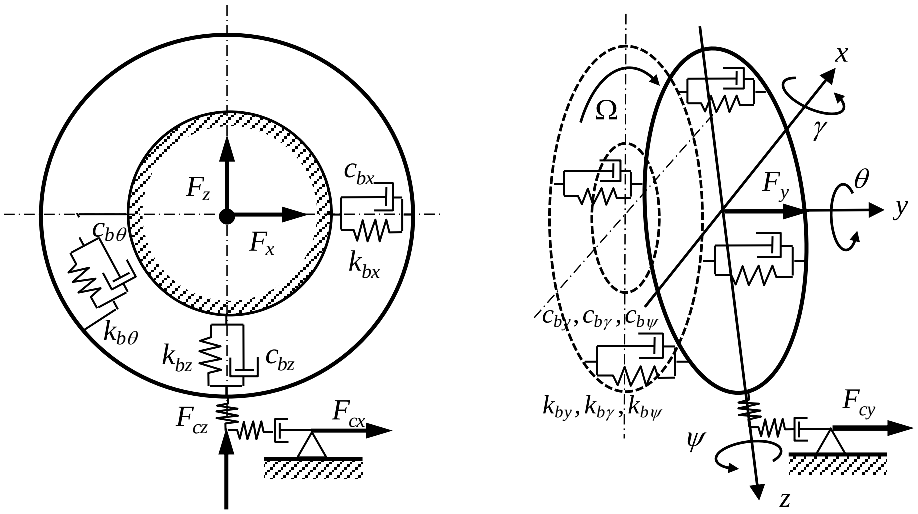

Figure 1 : Rigid ring model (SWIFT model)

2.2 Equations of motion

The wheel has three degrees freedom in translational motion : the vertical, longitudinal and lateral displacements and rotational motion about the axes perpendicular to the wheel plane. The equations of motion for the three translational motion of the wheel read:

$$\begin{aligned} F_x &= m_a \ddot{x}_a + c_{bx}(\dot{x}_a - \dot{x}_b) + k_{bx}(x_a - x_b) + c_{bz}\Omega(z_a - z_b) \\ F_y &= m_a \ddot{y}_a + c_{by}(\dot{y}_a - \dot{y}_b) + k_{by}(y_a - y_b) \\ F_z &= m_a \ddot{z}_a + c_{bz}(\dot{z}_a - \dot{z}_b) + k_{bz}(z_a - z_b) - c_{bx}\Omega(x_a - x_b) \end{aligned} \quad (1)$$

and the equation of motion for rotational motion of the wheel read:

$$M_{ay} = I_{ay}\ddot{\theta}_a + c_{b\theta}(\dot{\theta}_a - \dot{\theta}_b) + k_{b\theta}(\theta_a - \theta_b) \quad (2)$$

The tire ring has six degrees of freedom : three translational motion and three rotational motion. The equations of motion for translational motion of the tire ring read:

$$\begin{aligned} &m_b\ddot{x}_b + c_{bx}(\dot{x}_b - \dot{x}_a) + k_{bx}(x_b - x_a) + c_{bz}\Omega(z_b - z_a) = F_{cx} \\ &m_b\ddot{y}_b + c_{by}(\dot{y}_b - \dot{y}_a) + k_{by}(y_b - y_a) = F_{cy} \\ &m_b\ddot{z}_b + c_{bz}(\dot{z}_b - \dot{z}_a) + k_{bz}(z_b - z_a) - c_{bx}\Omega(x_b - x_a) = F_{cz} \end{aligned} \tag{3}$$

and the equations of motion for rotational motion of the tire ring read:

$$\begin{aligned} &I_{bx}\ddot{\gamma}_b + c_{b\gamma}\dot{\gamma}_b + k_{b\gamma}\gamma_b + c_{b\psi}\Omega\psi_b + I_{by}\Omega\dot{\psi}_b = -r_l F_{cy} - r_l\gamma_b F_{cz} + M_{cx} \\ &I_{by}\ddot{\theta}_b + c_{b\theta}(\dot{\theta}_b - \dot{\theta}_a) + k_{b\theta}(\theta_b - \theta_a) = r_e F_{cx} + M_{cy} \\ &I_{bz}\ddot{\psi}_b + c_{b\psi}\dot{\psi}_b + k_{b\psi}\psi_b + c_{b\gamma}\Omega\gamma_b + I_{by}\Omega\dot{\gamma}_b = M_{cz} \end{aligned} \tag{4}$$

where x_a, y_a, z_a are wheel (shaft) displacement and θ_a is the small derivation of the angular displacement of the wheel on the top of displacement due to steady speed of rotation Ω ; F_x, F_y, F_z are external force acting on the wheel (shaft) ; M_{ay} is the drive torque. x_b, y_b, z_b are tire belt displacement and $\gamma_b, \theta_b, \psi_b$ are derivation of angular displacement of the tire belt ; F_{cx}, F_{cy}, F_{cz} are lug excitation force generated at the tire-road interface ; M_{cx}, M_{cy}, M_{cz} are rolling resistance torque acting on the tire belt ; m_a and I_{ay} are the mass and moment of inertia of the wheel ; m_b and I_{bx}, I_{by}, I_{bz} are the mass and moment of inertia of the tire belt. As for tire sidewall damping, translational damping coefficient c_{bx}, c_{by}, c_{bz} and rotational damping coefficient $c_{b\gamma}, c_{b\theta}, c_{b\psi}$ are introduced. As for tire sidewall stiffness, translational stiffness k_{bx}, k_{by}, k_{bz} and rotational stiffness $k_{b\gamma}, k_{b\theta}, k_{b\psi}$ are introduced. Further, the interface between the tire belt and road surface is modelled by a contact patch slip model. In this slip model, the tire-road interface is represented by two first-order differential equations for the longitudinal and lateral direction

$$\begin{aligned} &\sigma_{cx}\dot{\varsigma}_{cx} + V_{cx}\varsigma_{cx} = -V_x - \dot{x}_b + r_e\dot{\theta}_b \\ &\sigma_{cy}\dot{\varsigma}_{cy} + V_{cx}\varsigma_{cy} = -V_y - \dot{y}_b + r_l\dot{\gamma}_b + V_x\psi_b \end{aligned} \tag{5}$$

where σ_{cx}, σ_{cy} are the contact patch relaxation length ; ζ_{cx}, ζ_{cy} are the slip in the contact patch ; V_{cx}, V_{cy} are the slip velocities in the contact patch ; V_x, V_y are the slip velocities at the wheel centre line ; r_e, r_l are the effective rolling radius and the loaded rolling radius.

Next, the equations of motion of the tire ring are arranged in order to obtain the natural frequencies and the natural modes analytically in the condition of non-rotating and with the ground contact. To study the behaviour of the tire belt with respect to the wheel, the motions of the wheel are constrained to zero: $x_a = y_a = z_a = 0$ and non-rotating leads to $\Omega = 0$. Further, the equations of motion are linearized by introducing the state variables as small variations additional to the stationary values which represent the considered undisturbed state of operation $\tilde{\theta}_a, \tilde{x}_b, \tilde{y}_b, \tilde{z}_b, \tilde{\gamma}_b, \tilde{\theta}_b, \tilde{\psi}_b, \tilde{F}_{cx}, \tilde{F}_{cy}, \tilde{F}_{cz}$. From the Eq. (3),(4) and (5), it appears that the in-plane and out-of-plane dynamics are independent each other. That means that the in-plane and out-of-plane dynamics of the ring model can be treated separately. Therefore, the equations of motion are rearranged to describe the in-plane and the out-of-plane dynamics of the rigid ring model. The set of equations for the in-plane tire dynamics read:

$$\begin{aligned} &m_b\ddot{\tilde{x}}_b + c_{bx}\dot{\tilde{x}}_b + k_{bx}\tilde{x}_b + c_{bz}\Omega\tilde{z}_b = \tilde{F}_{cx} \\ &m_b\ddot{\tilde{z}}_b + c_{bz}\dot{\tilde{z}}_b + k_{bz}\tilde{z}_b - c_{bx}\Omega\tilde{x}_b = \tilde{F}_{cz} \\ &I_{by}\ddot{\tilde{\theta}}_b + c_{b\theta}(\dot{\tilde{\theta}}_b - \dot{\tilde{\theta}}_a) + k_{b\theta}(\tilde{\theta}_b - \tilde{\theta}_a) = -r_{e0}\tilde{F}_{cx} \\ &I_{ay}\ddot{\tilde{\theta}}_\omega + c_{b\theta}(\dot{\tilde{\theta}}_a - \dot{\tilde{\theta}}_b) + k_{b\theta}(\tilde{\theta}_a - \tilde{\theta}_b) = 0 \\ &\sigma_{cx}\dot{\tilde{\varsigma}}_{cx} + V_{cx}\tilde{\varsigma}_{cx} = -\dot{\tilde{x}}_b + r_{e0}\dot{\tilde{\theta}}_b \end{aligned} \tag{6}$$

while the out-of-plane tire dynamics are described by

$$\begin{aligned}
&m_b\ddot{\tilde{y}}_b + c_{by}\dot{\tilde{y}}_b + k_{by}\tilde{y}_b + c_{bz}\Omega\tilde{z}_b = \tilde{F}_{cy} \\
&I_{bx}\ddot{\tilde{\gamma}}_b + c_{b\gamma}\dot{\tilde{\gamma}}_b + k_{b\gamma}\gamma_b + c_{b\psi}\Omega\tilde{\psi}_b + I_{by}\Omega\dot{\tilde{\psi}}_b = -r_{l0}\tilde{F}_{cy} - r_{l0}\tilde{\gamma}_b F_{cz0} \\
&I_{bz}\ddot{\tilde{\psi}}_b + c_{b\psi}\dot{\tilde{\psi}}_b + k_{b\psi}\tilde{\psi}_b + c_{b\gamma}\Omega\tilde{\gamma}_b + I_{by}\Omega\dot{\tilde{\gamma}}_b = -t_0\tilde{F}_{cy} \\
&\sigma_{cy}\dot{\tilde{\varsigma}}_{cy} + V_{cx}\tilde{\varsigma}_{cy} = -\dot{\tilde{y}}_b + r_{l0}\dot{\tilde{\gamma}}_b + V_x\tilde{\psi}_b
\end{aligned} \tag{7}$$

in which r_{e0}, r_{l0}, t_0 and F_{cz0} are the stationary components of the radius, the pneumatic trail and the vertical force respectively. The expression of the variation of the lug excitation force in the contact patch read:

$$\tilde{F}_{cx} = K_{cx}\tilde{\varsigma}_{cx}\ ,\ \tilde{F}_{cy} = K_{cy}\tilde{\varsigma}_{cy}\ ,\ \tilde{F}_{cz} = k_{cz}\tilde{z}_b \tag{8}$$

where K_{cx}, K_{cy} are slip stiffness in the contact patch and k_{cz} is the vertical residual stiffness. By substituting Eq. (8) into Eq. (6), (7), $\tilde{\zeta}_{cx}, \tilde{\zeta}_{cy}, \dot{\tilde{\zeta}}_{cx}, \dot{\tilde{\zeta}}_{cy}$ are eliminated and the equations for the in-plane tire dynamics give:

$$\begin{aligned}
&m_b\ddot{\tilde{x}}_b + c_{bx}\dot{\tilde{x}}_b + (k_{bx} + K_{cx}/\sigma_{cx})\tilde{x}_b - (r_{e0}K_{cx}/\sigma_{cx})\tilde{\theta}_b = 0 \\
&m_b\ddot{\tilde{z}}_b + c_{bz}\dot{\tilde{z}}_b + (k_{bz} + k_{cz})\tilde{z}_b = 0 \\
&I_{ay}\ddot{\tilde{\theta}}_\omega + c_{b\theta}(\dot{\tilde{\theta}}_a - \dot{\tilde{\theta}}_b) + k_{b\theta}(\tilde{\theta}_a - \tilde{\theta}_b) = 0 \\
&I_{by}\ddot{\tilde{\theta}}_b + c_{b\theta}(\dot{\tilde{\theta}}_b - \dot{\tilde{\theta}}_a) + (k_{b\theta} + r_{e0}^2K_{cx}/\sigma_{cx})\tilde{\theta}_b - k_{b\theta}\tilde{\theta}_\omega - (r_{e0}K_{cx}/\sigma_{cx})\tilde{x}_b = 0
\end{aligned} \tag{9}$$

and the equation for the out-of-plane tire dynamics are described by

$$\begin{aligned}
&m_b\ddot{\tilde{y}}_b + c_{by}\dot{\tilde{y}}_b + (k_{by} + K_{cy}/\sigma_{cy})\tilde{y}_b - (r_{l0}/\sigma_{cy})\tilde{\gamma}_b = 0 \\
&I_{bx}\ddot{\tilde{\gamma}}_b + c_{b\gamma}\dot{\tilde{\gamma}}_b + (k_{b\gamma} + r_{l0}^2K_{cy}/\sigma_{cy} + r_{l0}F_{cz0})\tilde{\gamma}_b - (r_{l0}K_{cy}/\sigma_{cy})\tilde{y}_b = 0 \\
&I_{bz}\ddot{\tilde{\psi}}_b + c_{b\psi}\dot{\tilde{\psi}}_b + k_{b\psi}\tilde{\psi}_b + (r_{l0}t_0K_{cy}/\sigma_{cy})\tilde{\gamma}_b - (t_0K_{cy}/\sigma_{cy})\tilde{y}_b = 0
\end{aligned} \tag{10}$$

2.3 Natural frequencies and natural modes

The in-plane and out-of-plane dynamics are independent each other. Therefore, natural frequencies and natural modes can be derived separately. As for in-plane dynamics, Eq. (9) are described by matrix form

$$M\underline{\ddot{x}} + C\underline{\dot{x}} + K\underline{x} = \underline{0} \tag{11}$$

$$\left.\begin{aligned}
&\underline{x} = \begin{bmatrix}\tilde{x}_b & \tilde{z}_b & \tilde{\theta}_a & \tilde{\theta}_b\end{bmatrix}^T \\
&M = \begin{bmatrix} m_b & 0 & 0 & 0 \\ 0 & m_b & 0 & 0 \\ 0 & 0 & I_{ay} & 0 \\ 0 & 0 & 0 & I_{by}\end{bmatrix} \quad C = \begin{bmatrix} c_{bx} & 0 & 0 & 0 \\ 0 & c_{bz} & 0 & 0 \\ 0 & 0 & c_{b\theta} & -c_{b\theta} \\ 0 & 0 & -c_{b\theta} & c_{b\theta}\end{bmatrix} \\
&K = \begin{bmatrix} k_{bx} + \dfrac{K_{cx}}{\sigma_{cx}} & 0 & 0 & -\dfrac{r_{e0}K_{cx}}{\sigma_{cx}} \\ 0 & k_{bz} + k_{cz} & 0 & 0 \\ 0 & 0 & k_{b\theta} & -k_{b\theta} \\ -\dfrac{r_{e0}K_{cx}}{\sigma_{cx}} & 0 & -k_{b\theta} & k_{b\theta} + \dfrac{r_{e0}^2K_{cx}}{\sigma_{cx}}\end{bmatrix}
\end{aligned}\right\} \tag{12}$$

In order to treat as eigenvalue problems, matrix forms are translated into

$$\mu^2 M\underline{x} + \mu C\underline{x} + K\underline{x} = \underline{0}$$
$$\Rightarrow \quad A\underline{\omega} = \mu\underline{\omega} \quad A = \begin{bmatrix} 0 & I \\ -M^{-1}K & -M^{-1}C \end{bmatrix} \quad \underline{\omega} = \begin{bmatrix} \underline{x} \\ \mu\underline{x} \end{bmatrix} \tag{13}$$

where matrix A read:

$$A = \left[\begin{array}{cccc:cccc} 0 & 0 & 0 & 0 & 1 & 0 & 0 & 0 \\ 0 & 0 & 0 & 0 & 0 & 1 & 0 & 0 \\ 0 & 0 & 0 & 0 & 0 & 0 & 1 & 0 \\ 0 & 0 & 0 & 0 & 0 & 0 & 0 & 1 \\ \hdashline -\frac{k_{bx}}{m_b} - \frac{K_{cx}}{m_b\sigma_{cx}} & 0 & 0 & \frac{r_{e0}K_{cx}}{m_b\sigma_{cx}} & -\frac{c_{bx}}{m_b} & 0 & 0 & 0 \\ 0 & -\frac{k_{bz}+k_{cz}}{m_b} & 0 & 0 & 0 & -\frac{c_{bz}}{m_b} & 0 & 0 \\ 0 & 0 & -\frac{k_{b\theta}}{I_{ay}} & \frac{k_{b\theta}}{I_{ay}} & 0 & 0 & -\frac{c_{b\theta}}{I_{ay}} & \frac{c_{b\theta}}{I_{ay}} \\ \frac{r_{e0}K_{cx}}{I_{by}\sigma_{cx}} & 0 & -\frac{k_{b\theta}}{I_{ay}} & -\frac{k_{b\theta}}{I_{by}} - \frac{r_{e0}^2K_{cx}}{I_{by}\sigma_{cx}} & 0 & 0 & \frac{c_{b\theta}}{I_{by}} & -\frac{c_{b\theta}}{I_{by}} \end{array}\right] \tag{14}$$

So, the natural frequencies and natural modes of the non-rotating tire with ground contact with respect to in-plane motion (rotational(in-phase), rotational(anti-phase), vertical and longitudinal) can be obtained by solving the eigenvalue and eigenvector of matrix A.

In similar way, as for out-of-plane dynamics, Eq. (10) can be described by matrix form

$$N\ddot{\underline{y}} + D\dot{\underline{y}} + S\underline{y} = \underline{0} \tag{15}$$

$$\left.\begin{array}{l} \underline{y} = \begin{bmatrix} \tilde{y}_b & \tilde{\gamma}_b & \tilde{\psi}_b \end{bmatrix}^T \\ N = \begin{bmatrix} m_b & 0 & 0 \\ 0 & I_{bx} & 0 \\ 0 & 0 & I_{bz} \end{bmatrix} \quad D = \begin{bmatrix} c_{by} & 0 & 0 \\ 0 & c_{b\gamma} & 0 \\ 0 & 0 & c_{b\psi} \end{bmatrix} \\ S = \begin{bmatrix} k_{by} + \frac{K_{cy}}{\sigma_{cy}} & -\frac{r_{l0}K_{cy}}{\sigma_{cy}} & 0 \\ -\frac{r_{l0}K_{cy}}{\sigma_{cy}} & k_{b\gamma} + \frac{r_{l0}^2K_{cy}}{\sigma_{cy}} + r_{l0}F_{cz0} & 0 \\ -\frac{t_0K_{cy}}{\sigma_{cy}} & \frac{r_{l0}t_0K_{cy}}{\sigma_{cy}} & k_{b\psi} \end{bmatrix} \end{array}\right\} \tag{16}$$

Similarly, matrix forms are translated into

$$\lambda^2 N\underline{y} + \lambda D\underline{y} + S\underline{y} = \underline{0}$$
$$\Rightarrow \quad B\underline{\xi} = \lambda\underline{\xi} \quad B = \begin{bmatrix} 0 & I \\ -N^{-1}S & -N^{-1}D \end{bmatrix} \quad \underline{\xi} = \begin{bmatrix} \underline{y} \\ \lambda\underline{y} \end{bmatrix} \tag{17}$$

where matrix B read:

$$B=\left[\begin{array}{ccc:ccc} 0 & 0 & 0 & 1 & 0 & 0 \\ 0 & 0 & 0 & 0 & 1 & 0 \\ 0 & 0 & 0 & 0 & 0 & 1 \\ \hdashline -\dfrac{k_{by}}{m_b}-\dfrac{K_{cy}}{m_b\sigma_{cy}} & \dfrac{r_{l0}K_{cy}}{m_b\sigma_{cy}} & 0 & -\dfrac{c_{by}}{m_b} & 0 & 0 \\ \dfrac{r_{l0}K_{cy}}{I_{bx}\sigma_{cy}} & -\dfrac{k_{b\gamma}}{I_{bx}}-\dfrac{r_{l0}^2K_{cy}}{I_{bx}\sigma_{cy}}-\dfrac{r_{l0}F_{cz0}}{I_{bx}} & 0 & 0 & -\dfrac{c_{b\gamma}}{I_{bx}} & 0 \\ \dfrac{t_0K_{cy}}{I_{bz}\sigma_{cy}} & -\dfrac{r_{l0}t_0K_{cy}}{I_{bz}\sigma_{cy}} & -\dfrac{k_{b\psi}}{I_{bz}} & 0 & 0 & -\dfrac{c_{b\psi}}{I_{bz}} \end{array}\right] \quad (18)$$

Natural frequencies and natural modes with respect to out-of-plane motion (camber, yaw, lateral) can be obtained by solving the eigenvalue and eigenvector of matrix B.

3. Parameter identification

3.1 Experimental modal analysis result

By the excitation test of non-rotating agricultural tire with ground contact, seven natural frequencies corresponding to rigid mode were confirmed [7]. The natural frequencies and natural modes are shown in Table 1.

Table 1 : Natural frequencies and natural modes

	Natural frequency	Natural mode
in-plane motion	48.0Hz	rotational mode (in-phase)
	68.5Hz	rotational mode (anti-phase)
	74.5Hz	vertical mode
	92.0Hz	longitudinal mode
out-of-plane motion	35.0Hz	camber mode
	39.0Hz	yaw mode
	84.5Hz	lateral mode

By using these natural frequencies, the parameters of the rigid ring model are identified as for in-plane and out-of-plane motion respectively.

3.2 Parameter identification

As for the unknown parameters of the rigid ring model, $c_{bx}, c_{bz}, c_{b\theta}, k_{bx}, k_{bz}, k_{b\theta}, K_{cx}, \sigma_{cx}, r_{e0}, k_{cz}$ are related to in-plane motion and $c_{by}, c_{b\gamma}, c_{b\psi}, k_{by}, k_{b\gamma}, k_{b\psi}, K_{cy}, \sigma_{cy}, r_{l0}, t_0$ are related to out-of-plane motion. As the known parameters, $m_b = 2.39$kg : $I_{ay} = 0.02$kgm^2 : $I_{bx} = I_{bz} = 0.012$kgm^2 : $I_{by} = 0.024$kgm^2, $F_{cz0} = 200$N are used. By assuming these unknown parameters, the natural frequencies can be calculated from the eigenvalue of Eq. (14) and Eq. (18). Therefore, the parameters are determined based on the optimization method so that the difference between the experimental and the calculated natural frequencies can be minimized. The error functions are defined as for in-plane and out-of-plane parameters respectively

$$Error(c_{bx}, c_{bz}, c_{b\theta}, k_{bx}, k_{bz}, k_{b\theta}, K_{cx}, \sigma_{cx}, r_{e0}, k_{cz}) = \sum_{n=1}^{4}\frac{\left\{f_n^{\exp} - f_n^{cal}\right\}^2}{\left\{f_n^{\exp}\right\}^2} \quad (19)$$

$$Error(c_{by}, c_{b\gamma}, c_{b\psi}, k_{by}, k_{b\gamma}, k_{b\psi}, K_{cy}, \sigma_{cy}, r_{l0}, t_0) = \sum_{n=1}^{3}\frac{\left\{f_n^{\exp} - f_n^{cal}\right\}^2}{\left\{f_n^{\exp}\right\}^2} \quad (20)$$

We use a non-linear optimization method, the Downhill Simplex method.

4. Identification results

The identified parameters are shown in Table 2.

Table 2 : Identified parameters

in-plane motion			out-of-plane motion		
Parameter	Unit	Value	Parameter	Unit	Value
c_{bx}, c_{bz}	Ns/m	1.38×10^3	c_{by}	Ns/m	1.21×10^3
$c_{b\theta}$	Nm s/rad	1.85×10	$c_{b\gamma}, c_{b\psi}$	Nm s/rad	6.06
k_{bx}, k_{bz}	N/m	3.84×10^5	k_{by}	N/m	2.81×10^5
$k_{b\theta}$	Nm/rad	7.67×10^3	$k_{b\gamma}, k_{b\psi}$	Nm/rad	1.41×10^3
K_{cx}	N	1.03×10^4	K_{cy}	N	6.37×10^2
σ_{cx}	m	6.73×10^{-2}	σ_{cy}	m	1.17×10^{-3}
r_{e0}	m	3.19×10^{-1}	r_{l0}	M	2.58×10^{-3}
k_{cz}	N/m	3.04×10^5	t_0	M	1.35×10^{-3}

Next, Table 3 lists the natural frequencies obtained from the experiment and those predicted by the calculations for in-plane and out-of-plane motions. Both results show good agreement. From these results, it is considered that the parameters are identified precisely.

Table 3 : Comparison of natural frequencies

	in-plane motion				out-of-plane motion		
Experiment	48.0Hz	68.5Hz	74.5Hz	92.0Hz	35.0Hz	39.0Hz	84.5Hz
Calculation	48.9Hz	68.4Hz	72.1Hz	91.6Hz	36.8Hz	36.7Hz	84.5Hz

Furthermore, each of eigenvectors corresponding to the natural frequencies are calculated and the natural modes are estimated. The calculated eigenvector and estimated natural mode are shown in Table 4 (in-plane motion) and Table 5 (out-of-plane motion) respectively.

Table 4 : Estimation of natural mode from eigenvector (in-plane motion)

Frequency		48.9Hz	68.4Hz	72.1Hz	91.6Hz
Eigenvector	$\tilde{x}_b$	-4.32×10^{-4}	-6.98×10^{-6}	2.49×10^{-19}	**6.98×10^{-5}**
	$\tilde{z}_b$	-1.05×10^{-18}	-1.61×10^{-19}	**9.99×10^{-4}**	-3.05×10^{-19}
	$\tilde{\theta}_a$	**-1.35×10^{-3}**	**-8.94×10^{-4}**	3.07×10^{-18}	3.53×10^{-4}
	$\tilde{\theta}_b$	**-9.65×10^{-4}**	**5.18×10^{-4}**	1.17×10^{-18}	-3.09×10^{-4}
Mode		rotational mode (in-phase)	rotational mode (anti-phase)	vertical mode	longitudinal mode

Table 5 : Estimation of natural mode from eigenvector (out-of-plane motion)

Frequency		36.8Hz	36.7Hz	84.5Hz
Eigen vector	$\tilde{y}_b$	-5.56×10^{-6}	-1.22×10^{-17}	**-6.34×10^{-4}**
	$\tilde{\gamma}_b$	**-2.16×10^{-3}**	-4.56×10^{-15}	-3.29×10^{-4}
	$\tilde{\psi}_b$	1.83×10^{-5}	**-2.16×10^{-3}**	1.72×10^{-4}
Mode		camber mode	yaw mode	lateral mode

In Table 4 and Table 5, the natural mode is estimated from the dominant component of eigenvector, where dominant component are described in bold. For example, the dominant component of eigenvector of 72.1Hz is $\tilde{z}_b$ vertical displacement. Therefore, the natural mode of 72.1Hz is estimated vertical mode.

The correspondence of the natural mode estimated from the eigenvector to the natural frequency coincides with the correspondence of the natural mode to the natural frequency obtained from the experiment shown in Table 1.

5. Conclusion

In this study, the agricultural tire is modelled as a rigid ring tire model, which is able to describe tire out-of-plane motion in order to estimate lateral lug excitation force. Then, the linearized equations of motion of the tire model are derived and the calculation procedure for obtaining the natural frequencies and natural modes is formulated. Furthermore, parameter identification method, where parameters estimated from the measured natural frequencies and the calculated natural frequencies by using optimizing method, is proposed. As a result, the natural frequencies and the natural modes predicted by the calculation using the identified model parameters show good agreement with those obtained experimentally. So the validity of the proposed optimization method is proved. Parameter identification of agricultural tire considering out-of-plane motion can be achieved by this technique.

REFERENCES

1 Fujita, K., Saito, T., and Kaneko, M. Influence of Vibration Characteristics on Dynamic Behaviour of Rolling Agricultural Tires, *Journal of the Japan Society of Agricultural Machinery (in Japanese)*, **71** (1), 124-130, (2011).

2 Fujita, K., Saito, T., and Kaneko, M. Study on dynamic characteristics of a rolling agricultural tire (Improvement of running condition), *Transaction of the Japan Society of Mechanical Engineers (in Japanese)*, **80** (812), 45-50, DOI:10.1299/transjsme.2014trans0065, (2014).

3 Fujita, K., Saito, T., and Kaneko, M. Study on dynamic characteristics of rolling agricultural tire (Identification of lug excitation force), *Transaction of the Japan Society of Mechanical Engineers (in Japanese)*, **82** (837), 1-8, DOI;10.1299/transjsme.15-00656, (2016).

4 Zegelaar, P. W. A., *The Dynamic Response of Tyres to Brake Torque Variations and Road Unevenness*, Ph.D. Thesis, Delft University of Technology, (1998).

5 Maurice, J. P., *The Short Wavelength and Dynamic Tyre Behaviour under Lateral and Combined Slip Condition to*, Ph.D. Thesis, Delft University of Technology, (2000).

6 Pacejka, H. B., *Tyre and Vehicle Dynamics*, Elsevier Ltd., Second Edition, (2006)

7 Fujita, K., Saito, T., and Kaneko, M. Experimental Research on Dynamic Characteristics of a Rolling Agricultural Tire (Measurement of Forces Acting on Tire Shaft), *Proceedings of the ASME International Mechanical Engineering Congress & Exposition*, Montreal, Canada, 14-20 November, (2014).